21 Basalt Street: Undercover mineral exploration of the Mount Read Volcanics in north-western Tasmania

George Taylor
Institute of Mine Seismology
george.taylor@imsi.org

Tjaart de Wit
Institute of Mine Seismology
tjaart.dewit@imsi.org

SUMMARY

The difficulty of searching for economically viable mineral deposits that occur beneath geological cover sequences has long driven innovation in exploration geophysics. Here, we present a case study of a novel passive seismic exploration technique that can be used to accurately image geological structure within the top 5 km of the Earth's crust. We deployed a dense array of 426 portable seismic sensors in the vicinity of Waratah in north-western Tasmania. This part of Tasmania has long been inferred to be underlain by Paleozoic basement rocks that contain the famed Mount Read Volcanics, a geological terrane that is highly prospective for volcanogenic massive sulphide deposits. To date, exploration near Waratah has been largely discouraged by the presence of a cover sequence of Paleogene basalt that is estimated to be up to 400 m thick in some locations. The presence of strong remanent magnetism in the basalt poses further difficulties to exploration efforts, and innovative geophysical methods are clearly required. To overcome the challenge posed by the thick cover sequence, we apply ambient noise surface wave tomography with the aim of creating a 3D S-wave velocity model of the top 4 km of the crust beneath the seismic array. Our seismic observations allow us to image the depth extent of the cover sequence, and identify a region of low seismic velocity (< 2.2 km/s) that likely corresponds to a pre-Paleogene topographic depression that contains a thick section of Paleogene basalt. Furthermore, we interpret a region of increased seismic velocity (> 2.5 km/s) as an area of thin basalt cover in the vicinity of the existing Hellyer mine site, as well as possible fault structures in the Paleozoic basement. We demonstrate that passive seismic methods can be effectively used to target follow-up geophysical studies of prospective areas even in the presence of thick geological cover.

Key words: Geophysics, Passive seismic, Mineral exploration, Tasmania, Mount Read Volcanics.

INTRODUCTION

Western Tasmania is famous for hosting a voluminous belt of felsic volcanic rocks that has become widely known to geologists as the Mount Read Volcanics (Campana and King, 1963). The volcanic pile is of middle Cambrian age ($\sim$535 to $\sim$525 Ma (Corbett, 1992)) and is generally thought to be the result of a period of extensional collapse that followed the collision of proto-Tasmania with an oceanic island arc in an event known as the Tyennan Orogeny. The Mount Read Volcanics generally form a north-striking, continuous belt approximately 10 km to 15 km wide that is closely associated with the western margin of the Precambrian nucleus of western Tasmania (Corbett, 1992).

The Mount Read Volcanics have a long history of economic importance to Tasmania, with six major volcanogenic massive sulphide deposits having been discovered within the belt to date at Mount Lyell, Rosebery, Hercules, Que River, Hellyer and Henty. Mining operations continue to the present day at Rosebery and Henty Gold Mine (Solomon, 1981). Vast areas of the volcanic belt remain relatively unknown and exploration activity in the region remains intense, with the primary focus being on areas located along strike from the known major deposits. Despite the prospectivity of large swathes of territory within the Mount Read Volcanics, geological exploration is generally hampered by factors such as high precipitation (> 2500 mm/yr) and the accompanying natural vegetation that consists of thick (sometimes impenetrable) temperate rainforest. Such environmental factors combine to not only severely restrict access to much of the volcanic belt, but also results in poor exposure of the underlying geology (Reid and Meares, 1981).

A further difficulty confronting exploration efforts within the Mount Read Volcanics is the complex geological and deformational history of western Tasmania. The Cambrian volcanic rocks and the accompanying mineral deposits have been extensively folded and faulted by a later deformation event in the late Cambrian and most prominently by the Devonian Tabberabberan Orogeny, which also coincided with the emplacement of large granitic plutons at a shallow crustal level (Seymour et al., 2014). The resulting deformation has resulted in great challenges for understanding the structure and stratigraphy of the Mount Read Volcanics.

The more recent geological history of Tasmania has included a significant amount of mafic volcanism since the late Cretaceous ($\sim$100 Ma), which is represented in north-western Tasmania by vast basalt lava fields (Seymour, 1981). Regional geological and airborne magnetic mapping suggest that a portion of the Mount Read Volcanics belt continues north beneath this basalt cover in the area north-west of Hellyer mine. Magnetic modelling of the basalt cover indicates an average thickness of 200 m above the Paleozoic basement rocks (Leaman, 1986), but stratigraphic boreholes drilled by Mineral Resources Tasmania indicate basalt cover in excess of 300 m near the town of Waratah (Baillie et al., 1987). The thick cover sequence of Paleogene basalt has to date largely discouraged further exploration, and it is clear that the development of novel, cost-effective geophysical methods is necessary before significant effort can be expended on exploration of this northern extension of the Mount Read Volcanics.

This study details the application of passive seismic imaging methods to a ~ 481 km^2 area in the vicinity of Waratah in north-western Tasmania (Fig. 1). The study area encompasses the region of the Paleogene basalt plateau that is expected to be underlain by Paleozoic basement rocks, including the northern extension of the Mount Read Volcanics. We deployed a dense regional network of portable seismic sensors that recorded approximately one month of continuous ground motion. In this paper we detail the application of ambient noise surface wave tomography to the continuous seismic data. We aim to construct a 3D S-wave velocity model of the top $\sim$4 km of the Earth's crust in north-west Tasmania. The S-wave velocity model will provide critical information on the deep geological structure of the area. In particular, the S-wave velocity model may be used to infer the thickness of the Paleogene basalt cover, and indicate prospective areas for follow-up geophysical surveys. Furthermore, our surface wave observations are directly sensitive to structures that are present in the Paleozoic rocks, and we are able to detect several linear features in the velocity model that may represent pre-Paleogene faults that affect the basement geology.

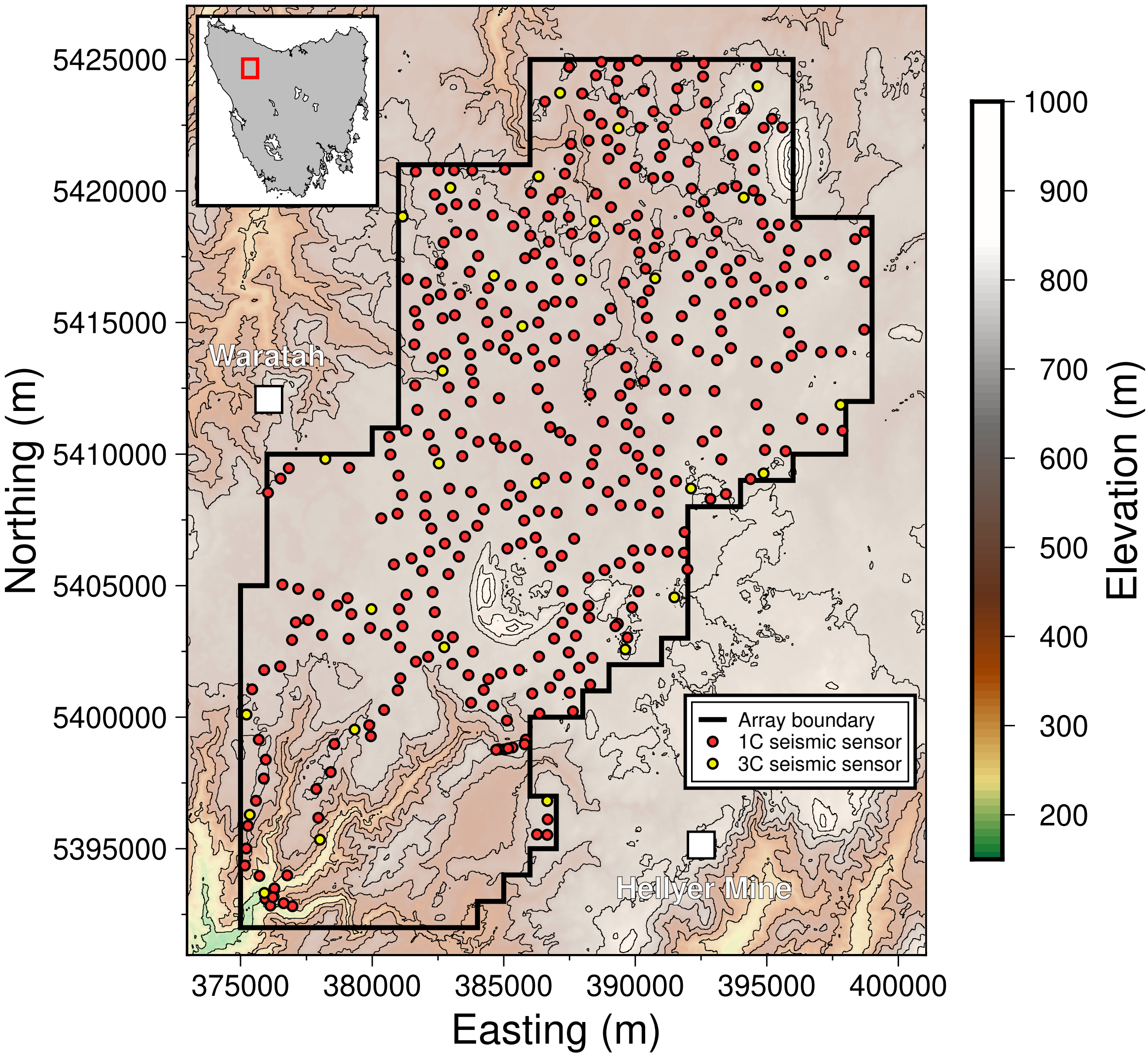

Figure 1. Regional overview of the passive seismic array used in this study. The inset map shows the location of the main map within Tasmania. The solid black line shows the boundary of the seismic deployment. Red circles are the locations of vertical component seismic sensors. Yellow circles show the locations of 3C seismic sensors. White squares indicate the localities of Waratah and Hellyer Mine. Topographic data is from the Shuttle Radar Topography Mission (Farr et al., 2007).

METHODOLOGY

Deployment of the passive seismic array

A regional array of portable seismic sensors was deployed in the Waratah-Guildford area of north-western Tasmania (Fig. 1) by staff from the Institute of Mine Seismology (IMS) during June 2023. Access to the majority of the region, particularly over the Paleogene basalt plain, is achieved by well-maintained forestry tracks. Access to the remote south-western portion of the seismic array is more difficult as fewer vehicle tracks are available. For the south-western sector, seismic equipment was carried in on foot. The seismic array instrumentation was a combination of 396 SmartSolo IGU-16 vertical-component sensors and 30 SmartSolo IGU-16 3-component sensors. Data recording by the seismic array was activated on June 9th 2023, and continued until the battery life of the equipment was exceeded after approximately 28 days. IMS staff returned to collect the seismic sensors by October 13th 2023.

Ambient noise data processing

Following the field deployment, the ground motion recordings were retrieved from the seismic sensors. The recordings at each sensor are first cut to 24-hour-long segments, which are down-sampled from the native sampling rate of 500 Hz to 20 Hz to improve the computational efficiency of the subsequent processing. After down-sampling, the ground motion records are split into 1-hour-long segments from which any linear trend in the data is removed, and a taper is applied to each end of the records to smooth the amplitudes to zero. The records are then band-pass filtered between 0.5 Hz and 5.0 Hz. In this study, we focus on the analysis of the vertical-component ground motion records recorded during the experiment.

After preparation of the raw waveform data, we applied the standard pre-processing for producing ambient noise cross-correlation functions from continuous seismic data (Bensen et al., 2007). The frequency spectrum of each 1-hour-long noise record is first ‘whitened’ to increase the relative contribution of low-amplitude noise sources to the record. The whitening is achieved by dividing the amplitude frequency spectrum of the noise record by a smoothed version of itself within the whitening window. The whitening window used in this study was 0.5 Hz to 5.0 Hz. To further reduce the disproportionate impact of high-amplitude noise sources on the cross-correlation process, time-domain amplitude normalisation of the seismic records is also required. To achieve this, we apply ‘one-bit’ normalisation of the whitened noise records. In one-bit normalisation, each sample in the seismic record is divided by its value, leaving the sample with a value of either 1 or -1. The one-bit normalisation process discards the amplitude information of the signal, but preserves the phase spectrum.

Subsequent to waveform pre-processing, 1-hour-long record seismic records at each seismic sensor were cross-correlated with the contemporaneous recording at every other sensor within the network. Data from the 426 retrieved sensors produce a total of 90,525 unique sensor pairs for cross-correlation. The individual 1-hour cross-correlation functions are then stacked for each sensor pair to produce the average cross-correlation function, which is assumed to be representative of the empirical Green’s function between the two sensors (Wapenaar, 2004). The overall effect is to obtain a ground motion record that represents the seismic waves that would be recorded at one of the sensors if an impulsive source such as dynamite had been initiated at the position of the other receiver.

Rayleigh wave group velocity extraction

The vertical component of the Earth’s seismic ambient noise field is dominated by elliptical surface waves known as Rayleigh waves. Thus, the dominant seismic phase present on empirical Green’s functions obtained by cross-correlating vertical component ground motion records is the Rayleigh wave. To extract estimates of Rayleigh wave group velocity at various propagation frequencies from the empirical Green’s functions we apply frequency-time analysis (FTAN). The FTAN method is described in detail by (Levshin and Ritzwoller, 2001) and (Bensen et al., 2007), and will only be briefly examined here. Each of the empirical Green’s functions is subjected to a series of narrow Gaussian band-pass filters with different centre frequencies. For each Gaussian filter, the arrival time of the maximum in the envelope of the band-pass filtered signal is calculated, as well as the instantaneous frequency of envelope maximum. The corresponding group speed for this instantaneous frequency is calculated by combining the group travel-time and the inter-station distance. The candidate group velocity at each frequency is then presented to the user, who manually picks the correct dispersion curve for the given sensor pair.

Rayleigh wave group velocity tomography

By combining the measurements of Rayleigh wave group velocity as a function of frequency for unique station pairs within the array, we are able to perform a seismic tomographic inversion to produces 2D maps of Rayleigh wave group velocity variation across the seismic array. We calculate group velocity maps at regular intervals in the frequency range 0.5 Hz to 2.0 Hz. To construct the group velocity maps, we invert the pair-wise frequency-dependent Rayleigh wave travel-time measurements through a process known as Hierarchical Bayesian Transdimensional Tomography (Bodin et al., 2012). Details of our tomographic approach can be found in Bodin et al. (2012), but in general, the tomographic process is conducted in an iterative process in which trial group velocity models are generated in a pseudo-random fashion. At each iteration, the predicted Rayleigh wave group travel-times for each sensor pair for the proposed velocity model are calculated and compared with the observed travel-times. If the trial model is considered to fit the observations in a satisfactory manner, the model is accepted, and stored for later appraisal. If the model does not fit the observations, it is discarded. In the present study, we generated a total of 5,000,000 group velocity models for each frequency in this manner. The final group velocity maps are calculated by ensemble averaging each of the accepted velocity models.

RESULTS

Rayleigh wave group velocity variation

Rayleigh wave group velocity variation across the study area at three distinct frequencies (0.67 Hz, 0.98 Hz and 1.31 Hz) is shown in Fig. 2. In general, lower frequency waves are sensitive to Earth structure at greater depths. Several general features can be discerned from these preliminary group velocity maps. The first is the presence of low group velocity anomalies ($<$2.2 km/s) over the central

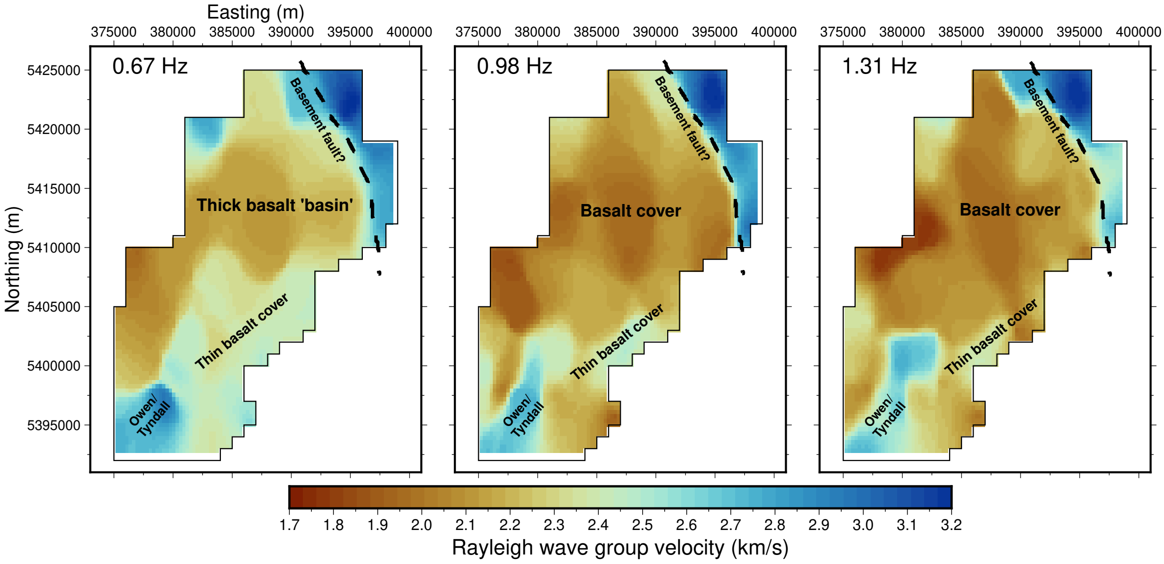

Figure 2. Interpreted Rayleigh wave group velocity variation across the area od the passive seismic deployment. Variation is shown at Rayleigh wave frequencies of 0.67 Hz, 0.98 Hz and 1.31 Hz. Warm colours indicate regions of slower Rayleigh wave group velocities, whereas blue colours indicate faster propagation speeds. The figure is annotated with geological interpretations discussed in the text.

portion of the seismic array at all frequencies. In contrast, much higher group velocity (>3.0 km/s) regions are located in the north-eastern and south-western parts of the study area.

In the north east, the high velocity anomaly is generally broad, and appears to terminate sharply against the central low velocity anomaly, with the contact between the two anomalies appearing to be relatively straight, striking south-east to north-west. The south-western high velocity anomaly appears to be more elongate, striking generally north-east to south-west, and is possibly associated with a broad region of moderate group velocities ($\sim$2.5 km/s) located in the south-eastern portion of the study area that is observed at 0.67 Hz.

Interpretation

Fig. 2 is annotated with several interpretations that may be drawn from the Rayleigh wave group velocity maps. We infer that the dominant low group velocity anomaly in the central portion of the seismic array is the result of the presence of the Paleogene-Neogene basalt cover that overlies the Paleozoic basement rocks. The persistence of this low velocity anomaly at low frequencies provides a qualitative indication of the thickness of the basalt cover. As such, the group velocity variation at 0.67 Hz can be interpreted to show a roughly circular region of thick basalt cover in the north-central portion of the licence area. The circular low velocity anomaly is approximately located between the localities of Waratah in the west, and Guildford in the east. We interpret the low velocity feature as representing a thicker than average sequence of Paleogene-Neogene basalt, perhaps indicating that the basalt was erupted into a pre-Paleogene topographic depression.

Fig. 2 also shows that the south-eastern section of the study area is characterised by elevated group velocity when compared with the northern and western portions. These elevated group velocities are particularly prominent at 0.67 Hz, and likely represent regions of abnormally thin basalt cover, where the Paleozoic basement rocks are located closer to the Earth's surface. This interpretation is supported by the observation that the south-eastern high velocity anomalies are closely associated with the further increased group velocity measurements in the south-western sector of the seismic array, where no basalt cover exists and Paleozoic basement rocks outcrop at the surface. The high group velocities (>3.0 km/s) in the south-western portion of seismic array are closely associated with the absence of Paleogene-Neogene basalt cover, and the outcrop of Paleozoic geological units that have been mapped as the Owen and Tyndall Groups. We interpret the high group velocity anomalies in the south-eastern sector to represent extensions possible of the Owen and Tyndall Group rocks beneath thin Paleogene-Neogene basalt.

The highest group velocity observations (up to 3.2 km/s, Fig. 2) are located in the far north-eastern portion of the seismic array. It is clear that, similar to the south-western sector, these elevated group velocities are associated with a lack of basalt cover and exposed Paleozoic basement rocks in the vicinity of Saint Valentines Peak. An intriguing aspect of the north-eastern group velocity anomaly is the sharp, straight nature of the contact with the low velocity anomaly associated with Paleogene-Neogene basalt. The group velocity maps indicate that the position of the south-east striking contact between the velocity anomalies may lie beneath basalt cover. One possible interpretation for the nature of this contact is that it represents a pre-Paleogene fault structure that has brought the older Paleozoic rocks closer to the surface to the north-east of the contact, and down-thrown the Paleozoic to the south-west. We theorise that the down-thrown south-western portion of the Paleozoic sequence may have provided accommodation space for the thick basalt cover found south-west of the contact.

CONCLUSION

Ambient noise surface wave tomography is one of the key modern geophysical techniques that enables us to gain insights into deep geological structure. In this study, we have presented the results of a surface wave tomography study using data from an extremely dense array of seismic sensors that was deployed in north-western Tasmania. Our work has has demonstrated the application of passive seismic methods to the imaging of a prospective mineral terrane that is located beneath a thick cover sequence of Paleogene basalt lava fields.

Our analysis of Rayleigh wave group velocity variation has highlighted regional geological structures that are present beneath seismic array. Rayleigh wave group velocity variation shown in Fig. 2 show that the Paleogene-Neogene basalt cover manifests as anomalously low group velocity when compared with the Paleozoic basement rocks that include the Mount Read Volcanics. The association between the basalt cover and low group velocities has allowed us to interpret a much thicker cover sequence of basalt in the western sector of the seismic compared to the eastern portion. The Waratah-Guildford district in particular appears to contain a thick sequence of Paleogene-Neogene basalt in an approximately ‘basin’-like morphology which may represent a pre-Paleogene topographic depression such as a lake. By contrast, we infer thinner basalt cover in the south-eastern region of the study area which is located north-west of Hellyer mine. We anticipate that the further inversion of our Rayleigh wave group velocity observations to produce a 3D S-wave velocity model of the top 4 km of the Earth’s crust will provide more rich information about the subsurface geology. In particular, we expect to be able to construct an estimate of the structure of the pre-Paelogene unconformity surface at the base of the basalt cover to provide the depth to Paleozoic basement rocks. Furthermore, we anticipate the the 3D S-wave velocity model will also enable the interpretation of the seismic structure of the prospective Paleozoic rocks beneath the seismic array, including the delineation of major fault structures (e.g. Fig. 2).

ACKNOWLEDGMENTS

Ashley Morris, Richard Gillies and Robert Hill are gratefully acknowledged for their efforts in the field to deploy the passive seismic array.

REFERENCES

Baillie, P. W., Green, G. R., and Collins, P. L. F., Progress report on the Sub-basalt Drilling Project:, Technical report, Department of Mines Tasmania, 1987.

Bensen, G. D., Ritzwoller, M. H., Barmin, M. P., Levshin, A. L., Lin, F., Moschetti, M. P., Shapiro, N. M., and Yang, Y., 2007, Processing seismic ambient noise data to obtain reliable broad-band surface wave dispersion measurements: Geophysical Journal International, **169**, no. 3, 1239–1260.

Bodin, T., Sambridge, M., Rawlinson, N., and Arroucau, P., 2012, Transdimensional tomography with unknown data noise: Geophysical Journal International, **189**, no. 3, 1536–1556.

Campana, B., and King, D., 1963, Palaeozoic tectonism, sedimentation and mineralization in west tasmania: Journal of the Geological Society of Australia, **10**, no. 1, 1–53.

Corbett, K. D., 1992, Stratigraphic-volcanic setting of massive sulfide deposits in the Cambrian Mount Read Volcanics, Tasmania: Economic Geology, **87**, no. 3, 564–586.

Farr, T. G., Rosen, P. A., Caro, E., Crippen, R., Duren, R., Hensley, S., Kobrick, M., Paller, M., Rodriguez, E., Roth, L., Seal, D., Shaffer, S., Shimada, J., Umland, J., Werner, M., Oskin, M., Burbank, D., and Alsdorf, D., 2007, The shuttle radar topography mission: Reviews of Geophysics, **45**.

Leaman, D. E., Mount Read Volcanics Project: Preliminary interpretation and evaluation report, 1981 West Tasmania aeromagnetic survey.:, Technical report, Department of Mines Tasmania, 1986.

Levshin, A. L., and Ritzwoller, M. H., 2001, Automated detection, extraction, and measurement of regional surface waves: Pure and Applied Geophysics, **158**.

Reid, K. O., and Meares, R. M. D., 1981, Exploration for volcanic-hosted sulfide deposits in western Tasmania: Economic Geology, **76**, no. 2, 350–364.

Seymour, D. B., McClenaghan, M. P., Green, G. R., Everard, J. L., Berry, R. F., Callaghan, T., Davidson, G. J., and Hills, P. B., 2014, Mid-Paleozoic orogenesis, magmatism and mineralisation:, *in* Geological Evolution of Tasmania. Geological Society of Australia, 273–362.

Seymour, D. B., St Valentines, Tasmania. Geological Atlas 1:50,000 Series. Geological Survey Explanatory Report:, Technical report, Department of Mines Tasmania, 1981.

Solomon, M., 1981, An introduction to the geology and metallic ore deposits of Tasmania: Economic Geology, **76**, no. 2, 194–208.

Wapenaar, K., 2004, Retrieving the elastodynamic green’s function of an arbitrary inhomogeneous medium by cross correlation: Physical Review Letters, **93**.